IOP Conf. Series: Materials Science and Engineering **143** (2016) 012014 doi:10.1088/1757-899X/143/1/012014

Controlling pool depth during VAR of Alloy 718

F Lopez[1], J Beaman[1], R Williamson[1], D Evans[2]
[1] Department of Mechanical Engineering, University of Texas at Austin, Austin, TX 78705, USA
[2] Special Metals Corporation, New Hartford, NY 13413, USA

E-mail: felipelopez@utexas.edu

Abstract. A longtime goal of superalloy producers has been to control the geometry of the liquid pool in solidifying ingots. Accurate pool depth control at appropriate values is expected to result in ingots free of segregation defects. This article describes an industrial VAR experiment in which a 430mm (17 in) diameter Alloy 718 electrode was melted into a 510mm (20 in) ingot. In the experiment, the depth of the liquid pool at the mid-radius was controlled to three different set-points: 137 mm (nominal), 193 mm (deep) and 118 mm (shallow). At each level, the pool depth was marked by a power cutback of several minutes. The ingot was sectioned and longitudinal slices were cut out. Analysis of the photographed ingot revealed that accurate control was obtained for both the nominal and deep pool cases, while the third one was not conclusive.

1. Introduction

Alloy 718, a nickel-based superalloy, is the most widely-used superalloy in history. This material can be found extensively in aircraft engines and power-generation turbines. These days, the drive for increased operating efficiency in these applications has resulted in the need for larger, yet structurally ingots for forging stock of Alloy 718 [5]. However, this task has proved challenging due to an increasing tendency for segregation defects at larger diameters.

Engineers have dedicated years to the development of techniques to prevent segregation defects in large ingots of nickel superalloys. Triple melting (TM) by VIM+ESR+VAR was largely successful in that task and enabled the fabrication of ingots up to 510 mm (20 in) in diameter for Alloy 718 and 910 mm (36 in) for Alloy 706 [4]. Moreover, adjustments in chemistry (reducing carbon, nitrogen, and niobium) enabled the production of Alloy 718 ingots up to 910 mm (36 in) in diameter [6].

At the same time, it was observed that the tendency for defect formation in superalloys was determined by the liquid pool profile and ingot solidification patterns during the process. Based on this observation, it was hypothesized that accurate solidification control would result in improved ingots, and potentially larger Alloy 718 ingots free of segregation defects. However, the lack of an appropriate solidification model in VAR prevented the development of a pool profile controller.

The first attempt to control pool shape in VAR was reported by Beaman *et al.*[1].Although promising, the method was not extendable to large ingots due to the model's inability to describe convective heat transfer in the liquid phase. This paper describes the first pool depth control demonstration in large ingots. In the experiment, an alternative form of the controller proposed by Beaman was used to melt a 430 mm (17 in) diameter Alloy 718 electrode into a 510 mm (20 in) ingot.

The ingot was sectioned and Canada etched to reveal the pool shape profile, which compared favorably to the process set-points.

2. Controller design

The layout of the pool depth control system is depicted in Figure 1.Two reference signals are given to the process controller: a reference pool depth $S_{p,ref}$ and a reference electrode gap G_{ref}. The controller returns two commands: melting current I and ram drive speed V_{ram}, which are obtained by comparing the references to state estimates. Commanded current, drive speed, and several measurements from the furnace (electrode gap G, ram position X, current I, electrode mass M and voltage V) are fed to an electrode estimator, that returns estimates of melting efficiency μ_e[1]; electrode gap G_e; and bias in measured voltage and current, $U_{b,e}$ and $I_{b,e}$. Estimated melt rate MR_e is calculated from these parameters and fed to BAR[2] along with current I, voltage V and cooling gas (helium) pressure p_{he} to obtain predictions of the liquid pool profile $S_{p,BAR}$. These predictions are fed to an ingot estimator that returns estimates of the thermal state of the solidifying ingot. Estimates from both estimators are used by the controller to compute optimal control signals.

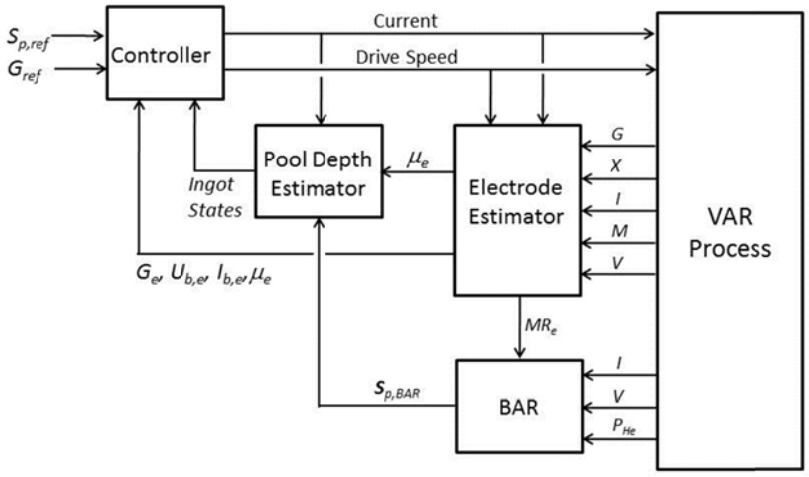

Figure 1. Schematic of the VAR pool depth controller design.

In this application, the process controller consists of two separate sub-systems: an electrode gap controller based on drive speed and a pool depth controller based on melting current. Commanded ram drive speed is set by a proportional controller following the design described in Ref. [2]. Meanwhile, commanded current is given by a Linear-Quadratic-Gaussian (LQG) controller that adds a nominal value to corrections for the estimated state, defined reference, estimated melting efficiency, and helium pressure; similar to the design in Ref. [1].

In this version of the pool depth controller, the ingot solidification model was obtained from a first-order approximation for pool depth dynamics which compared favorably to more accurate models (see Figure 2[3]). This model is able to track pool depth in four locations during the melt: at the center (r = 0.00 R), quarter-radius (r = 0.25 R), mid-radius (r = 0.50 R), and three-quarter-radius (r = 0.75 R). However, for simplicity, only mid-radius pool depth is used for process control.

[1]Defined as the instantaneous fraction of supplied power that is used in melting the electrode $\mu = P_{melt} / P_{total}$.

[2] Basic Axisymmetric Remelting (BAR) is the SMPC VAR solidification model. It is used to obtain predictions of liquid pool depth based on electric and thermal parameters of the process [3].

[3]BAR, a finite volume model, was used as benchmark for ingot solidification.

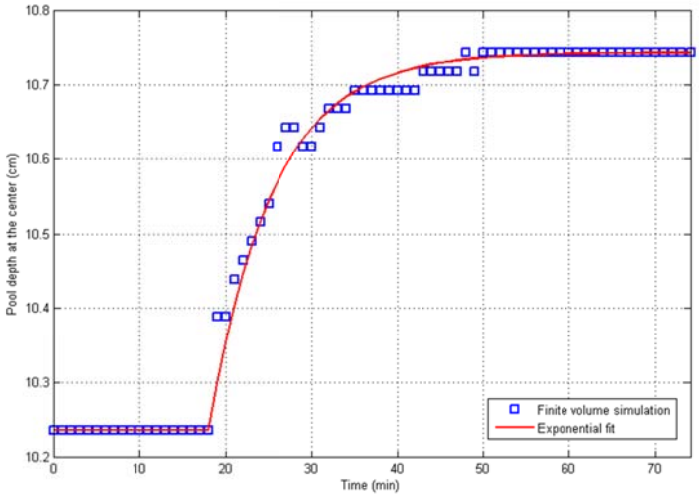

Figure 2. Comparison between BAR (finite volume simulation of ingot solidification) and a first-order exponential response for Alloy 718 in a 152 mm (6 in) to 203 mm (8 in) melt when current is instantaneously perturbed from 2500 A to 2750 A.

3. Experiment

The goal of the experiments was to test the proposed control strategy using SMPC's Advanced VAR Controller (AVARC)[4]. AVARC was run from a personal computer which communicated with the furnace control system through Ethernet connection. The experiment was carried out at Special Metals Corp. in New Hartford using a 430 mm (17 in) diameter electrode of Alloy 718, which was melted into a 510 mm (20 in) ingot.

In the experiment, the arc was struck with the host furnace PLC. Current was ramped up to a 6350 A hold. AVARC control was enabled after liquid metal was observed to cover the base plate. The initial control mode of the controller was set to current mode with a 6350 A set-point which was held for 240 minutes. This was followed by a change to pool depth mode with a mode transition time of 30 minutes.

Three mid-radius pool depths were programmed into the controller recipe: 137 mm (5.4 in), 193 mm (7.6 in) and 118 mm (4.6 in). The pool depth holds were separated by 90 minute ramps. Hot-top was programmed to begin with 227 kg of electrode remaining and involved ramping the pool depth down to 520 mm (2.5 in) over 90 minutes, followed by a 2500 A hold.

4. Experimental results

Figure 3 shows pool depth and current data for the entire test melt. The vertical dotted red line shows the point at which pool depth control mode was activated. Note the slight increase in current that occurs immediately after the switch, which is necessary to deepen the pool to the mid-radius set-point of 137 mm (5.4 in). The observed mid-radius liquid pool depth, measured with an online simulation of BAR, is plotted in blue and compared to the user-defined reference shown as black dash-dot line. Both lines coincide for nominal conditions and for the shallow pool case, but a mismatch of 7 mm can be observed for the deep pool one.

It is evident from these data that linear pool depth ramps defined in the reference require nonlinear current ramps. The three pool marking events are prominently evident in the current plot, as well as their effect in liquid pool depth.

[4]The Specialty Metals Processing Consortium (SMPC) is a collaborative program between several superalloy producers that conducts research on remelting processes.

The nonlinear current response that is required to produce agreement between the estimated pool depth and the reference set-point produces concomitant nonlinear responses in melt rate. This is seen in Figure 4 which shows plots of the estimated melt rate and measured pool depth (mid-radius). Note that during the first two pool marking events, melt rate is completely shut off, while it is reduced to about 340 g/min (0.75 lb/min) in the final pool marking event.

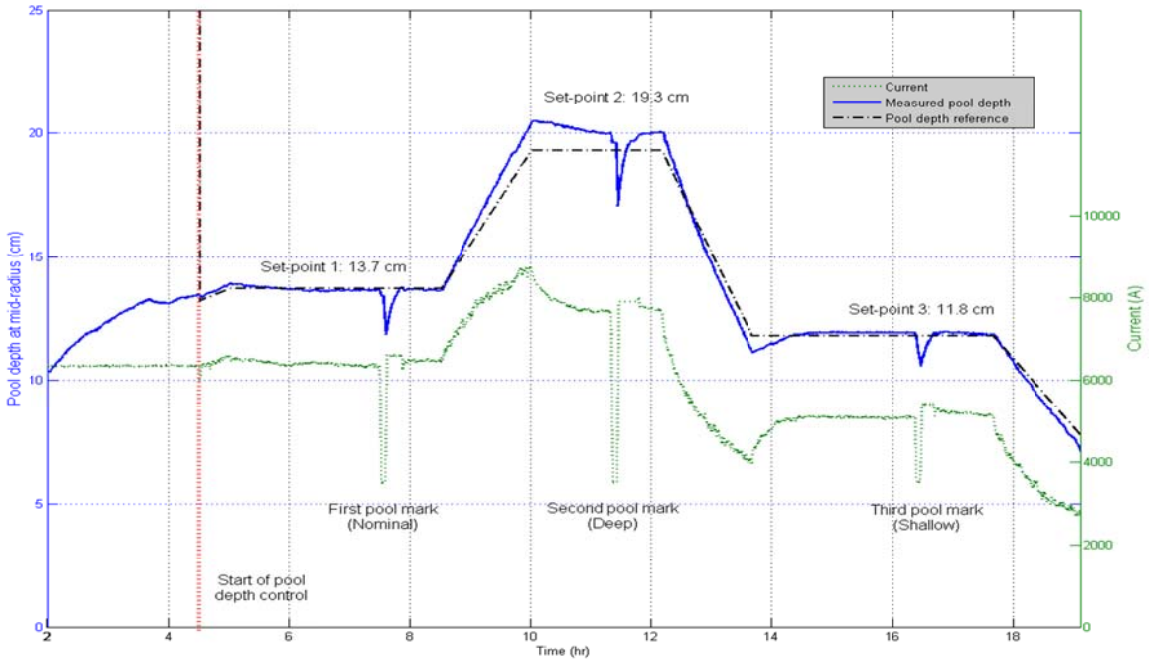

Figure 3. Overview of the test melt showing pool depth and commanded current.

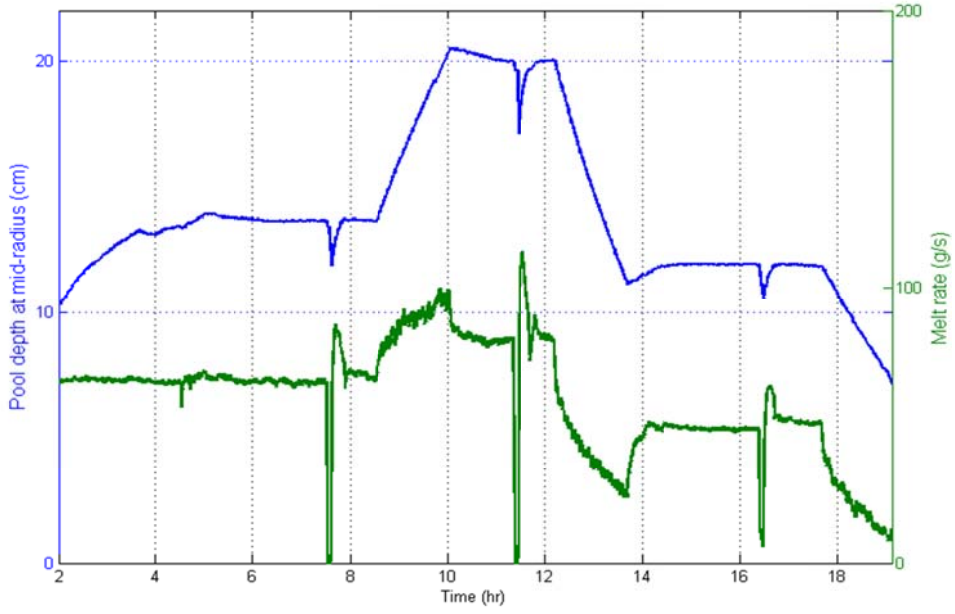

Figure 4. Comparison of pool depth and melt rate in the test melt.

Figure 5 (right) shows an expanded view of the current and electrode mass during the first pool marking event. It is evident from these data that the ingot does not grow significantly during the pool marking event. This is confirmed by the estimated melt rate data shown in Figure 5 (left). The estimated melt rate is zero by the time the minimum current of 3500 A is reached. Near the end of the low current hold it barely rises above zero. Integrating the regions where the current is ramped down and up gives ~ 4.7 kg (10.4 lbs) of electrode melted during this pool marking event, corresponding to ~3 mm (0.1 in) of ingot growth. Because this number is smaller than the error in determining the ingot height at the beginning of a pool marking event, the working assumption during the pool depth analysis is that the ingot does not grow during pool marking.

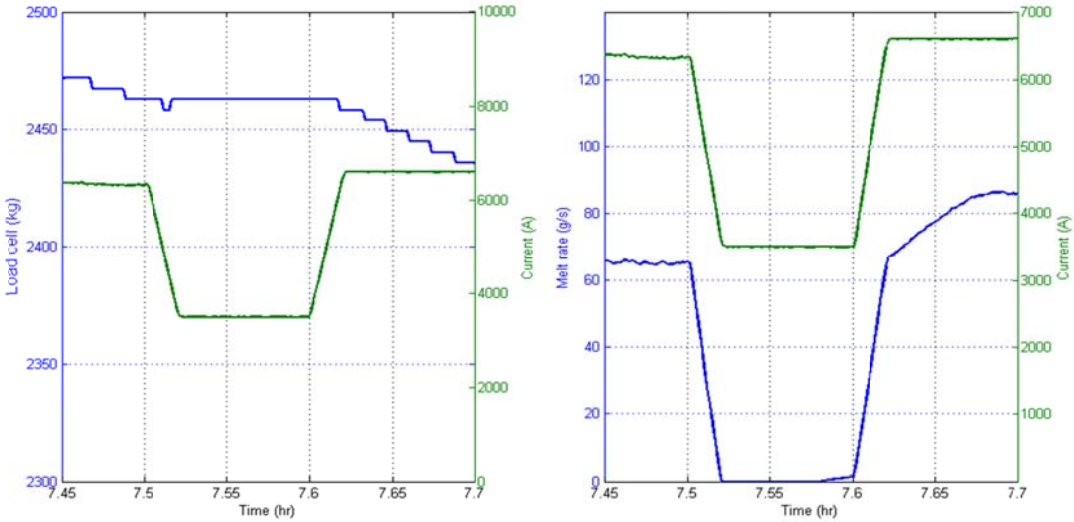

Figure 5. Expanded view of estimated melt rate, electrode mass and current during the first pool marking.

Given the large fluctuations in current and melt rate, as well as the violent perturbations introduced by the pool marking events, the question naturally arises as to how the controller performed with respect to drip-short based electrode gap control. Figure 6 shows plots of drip-short frequency, electrode gap calculated directly from the Zanner function using drip-short frequency and current, and the estimated electrode gap from the electrode estimator [7]. For this material and size, the Zanner function is given by $G=965.0 f_{DS}^{-0.595} I^{-0.669}$.

We note that "class zero" drip-shorts were used for gap control and that the ram was not allowed to back up during this trial. What stands out immediately from the plots is that the estimated electrode gap is very smooth and flat relative to the calculated electrode gap through all pool depth holds and ramps. This is in spite of large fluctuations in current and melt rate. Of course, the pool marking events are an exception to this, but even these are well behaved with maximum deviations of only about ±5 mm (±0.2 in). We conclude that gap was well controlled throughout the test melt. The exception to this is a large gap deviation that starts at about 18.1 hours at the end of the test[5].

Data presented in Figures 3-6 were obtained from the process controller. Besides these results, data were also obtained by cutting the test ingot into cylindrical sections, cutting sections in half longitudinally, and then cutting a plate from one of the longitudinal faces of each of the half sections. These sections were then Canada etched to reveal the segregation patterns on the face of each plate for the purpose of detecting the pool profiles generated by the pool marking events.

[5]This event was due to a ram position measurement problem that developed late in the melt and does not reflect controller performance.

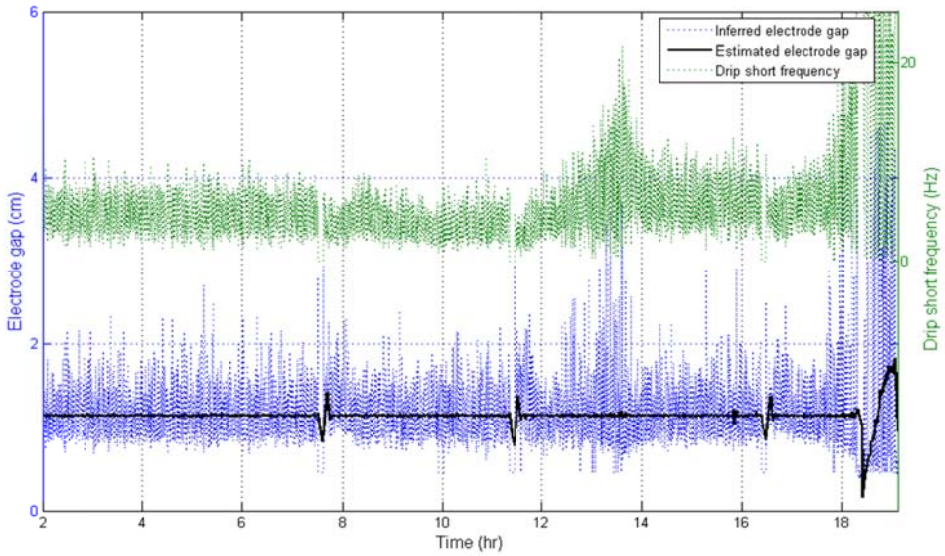

Figure 6. Plots of electrode gap inferred with Zanner's equation, estimated electrode gap, and drip short frequency for the test melt.

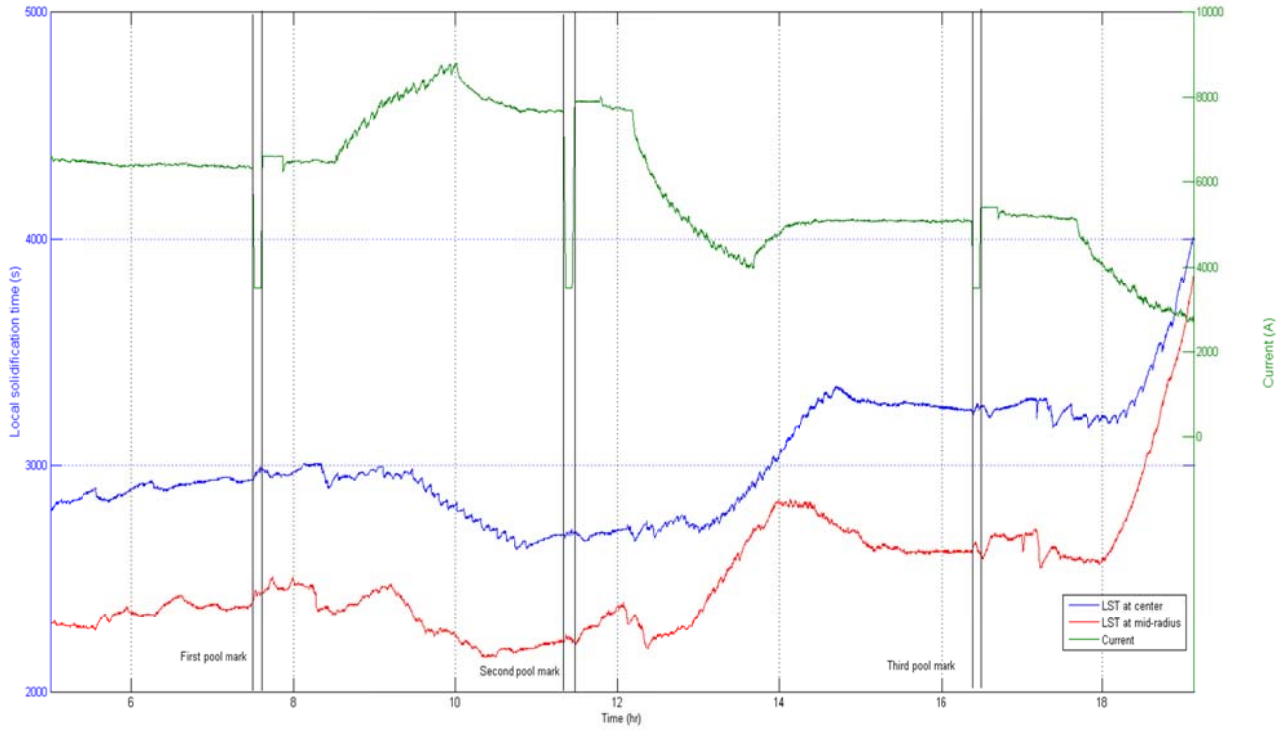

Figure 7. Local solidification time (LST) and current for the test melt.

Figure 7 shows a plot of local solidification time (LST) for the test, along with a plot of current. LSTs at the center and mid –radius were calculated by the controller during melting from BAR, the

finite volume model. The trend is as expected: the longest LST is in the center of the ingot and decreases toward the edge. Also the general trend is observed that LST decreases with increasing pool depth and increases with decreasing pool depth, with this trend most pronounced in the center of the ingot. Even though the mushy zone grows with increasing current, the casting rate also increases. It is evident from these data that BAR predicts that the increase in casting rate dominates LST determination under these casting conditions. Note that the perturbations from the pool marking events are felt first near the edge of the ingot and last at the center of the ingot.

Figure 8 (a) shows the results for the first pool marking. The event resulted in a smooth, relatively uniformly grey area with no evident "tree ring" banding. This presumably results from the pool solidifying in during the low power hold. The finite volume solution, shown by the red line in the figure, fits the bottom of this region very well; the mid-radius pool depth of 137 mm (5.4 in) is shown as the yellow line. A similar result is observed for the 193 mm (7.6 in) deep pool marking shown in Figure 8 (b). Both plates show evidence of heavy shelf forming during the low power hold.

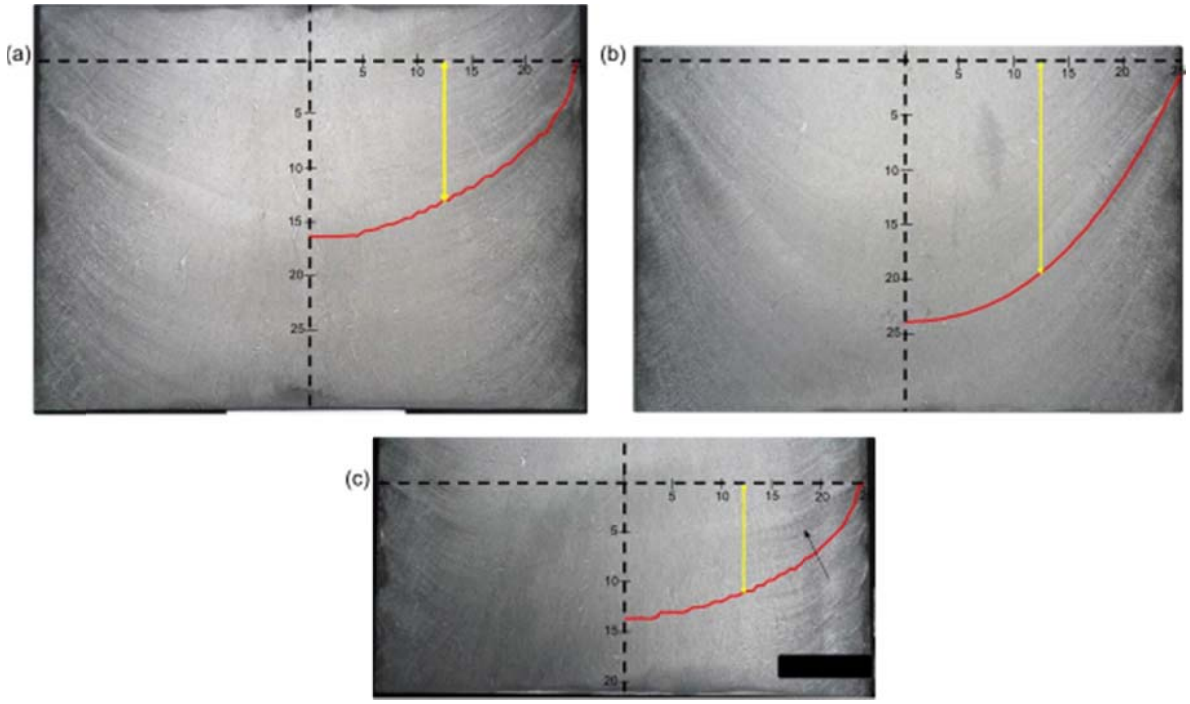

Figure 8.Finite volume pool depth measurement superimposed on an image of segregation (Canada) etched plate for references of: (a) 137 mm, (b) 193mm and (c) 118 mm (Scales in cm).

In spite of this success in controlling to the deeper pool shapes, the lines on the plate shown in Figure 8 (c) seem to indicate a much shallower pool than predicted by BAR or the controller. There is no clear indication of the location of the pool marking event. The black arrow points to light etching region but it is not conclusive. If this is the pool marking event, then the pool looks to be about 69 mm (2.7 in) deep at mid-radius instead of 118 mm (4.6 in). There is evidence of heavy shelf for this entire section of ingot and the photograph does not reveal any pool structure in the central region. More careful metallographic analysis may be required to actually determine the pool shape during the shallow pool depth hold.

5. Discussion

In general terms, the controller performed as it was designed to perform. It controlled the estimated mid-radius pool depth to the set-point reference and showed reasonable agreement with the finite volume predictions throughout the test. But, how well is this success reflected in the ingot structure?

The etching results for the first two commanded pool depths are particularly encouraging. Pool shapes revealed by the segregation patterns generally match BAR results and the mid-radius pool depths appear in reasonable agreement with the set-point values. Careful metallographic analysis of the plates will need to be performed if more accurate knowledge of the pool shapes is required, but the results shown in Figures 8 (a) and (b) are certainly very reasonable even if they are not perfectly accurate. Figure 8 (c), on the other hand, indicates a discrepancy between what was theoretically expected and what was actually produced in the ingot.

Going back to Figure 7, which shows calculated LSTs for the test melt, it is clear that a steady-state thermal distribution was not reached in the ingot during any of the pool depth holds. However, BAR data immediately prior to marking the 118 mm pool indicate that the solution is well behaved at this point. Given the evidence of heavy shelf in the segregation etched plate, it is possible that the shelf formed during the power cutback and simply never melted back at the relatively low power required to hold the shallow pool set-point (~5000 A). If this is true, we would expect the centerline pool depth to be closer to the BAR prediction. Confirmation (or refutation) of this hypothesis may be revealed by more careful metallurgical analysis of the plate.

The observation that pool depth may be controlled to a constant set-point under conditions of widely fluctuating LST indicates that this may not be the best solution to controlling the process so as not to form solidification defects. A better approach may be to control LST at one or more radial positions instead.

6. Conclusions

A VAR ingot pool depth controller was developed and successfully tested. A single industrial test was performed at Special Metals Corporation in New Hartford, New York. In the experiment, a 430 mm (17 in) diameter Alloy 718 electrode was remelted into a 510 mm (20 in) diameter ingot. Mid-radius ingot pool depth was controlled at three reference set-points during the test melt: 137 mm, 193 mm, and 118 mm. Post mortem analysis of the ingot revealed that control at the nominal and deep reference values was successfully implemented. Ingot analysis from the shallow pool depth was inconclusive. The relevant section of ingot shows signs of heavy shelf possibly left over from the power cutback required to produce the shallow pool depth set-point. What little information that can be gleaned from the ingot analysis indicates that the pool was significantly shallower than the 118 mm set-point, perhaps only 69 mm. Further more careful ingot analysis is warranted at this point.

In spite of the mismatch at the shallow pool depth setting, the controller performed successfully and predictably given the data that were being fed to it. This experiment constitutes the first successful pool depth control test in large ingots of Alloy 718. More testing will be required to determine safe pool depths to be used as references for the production of larger defect-free Alloy 718 ingots.

7. Acknowledgements

The author would like to thank the Specialty Metals Processing Consortium for support and Special Metals Corporation for hosting the experiment.

References

[1] Beaman J, Lopez F and Williamson R 2013 *J. Dyn. Syst.-T. ASME* **136(3)** 031007
[2] Beaman J, Williamson R, Melgaard D and Hamel J 2005 *Proc. IMECE* (Orlando, FL) p 1059
[3] Bertram L, Schunk P, Kempka S, Spadafora F and Minisandram R 1998 *JOM* **50(3)** p 18
[4] Moyer J, Jackman L, Adasczik C, David R and Forbes-Jones R 1994 *Proc. Superalloys 718, 625, 706 and various derivatives* (Warrendale, PA) p 39
[5] Schwant R, Thamboo S, Anderson A, Adasczik C, Bond B, Jackman L and Uginet J 1997 *Proc. Superalloys 718, 625, 706 and various derivatives* (Pittsburgh, PA) p 141
[6] Schwant R, Thamboo S, Yang L and Morra M 2005 *Proc. Int. Symp. Superalloys 718, 625, 706 and derivatives* (Pittsburgh, PA) p 15
[7] Zanner F 1981 *Met. Trans. B* **12(4)** p 721